

On Classification of MIMO Equalizers

Wing Chau Ng and Chuandong Li

Huawei Technologies, Ottawa, Canada, wing.chau.ng@huawei.com

Abstract Four classes of MIMO equalizers are presented based on a DSP-perceived model, with the corresponding partial or full channel inverses. The complete channel inverse shows a dependency on the complex conjugates of equalizer inputs, coinciding with the widely linear equalization theory.

Introduction

A decade ago, digital coherent optical receivers were primarily designed to undo the optical channel impairments, such as dispersion compensation (CD), polarization rotation, polarization mode dispersion (PMD), laser frequency offset (FO) and phase noise (PN) etc.^{[1],[2]}. These impairments take place on the optical fields, and therefore the digital signal processing (DSP) design was based on complex-valued inputs and complex-valued outputs, via adaptive equalizers using the ideal transmitted fields as references. As electrical impairments (such as s21 and phase mismatches, crosstalk) limit the next-generation coherent transceivers, it is indispensable to re-consider the overall channel starting from a four-dimensional (4D) real time-domain (TD) transmitted vector, $\tilde{t}_t = (i_{X,t}, q_{X,t}, i_{Y,t}, q_{Y,t})^T \in \mathbb{R}_t^{4 \times 1}$ to a 4D received vector, $\tilde{r}_t = (r_{X1,t}, r_{XQ,t}, r_{Y1,t}, r_{YQ,t})^T \in \mathbb{R}_t^{4 \times 1}$. Instead of a real physical model, one should consider the channel based on what the DSP can “perceive”.

In this theoretical work, the DSP-perceived channel is first simplified, based on which we categorize linear MIMO equalizers into four classes according to their reference locations. The entire channel inverse can be represented by a complex conjugate-dependent system, coinciding with the widely linear equalization theory^[3]. Suboptimally removing FO dynamics, relatively static channel inverses parameterized with common device and channel parameters are presented for monitoring or calibration purposes.

Channel perceived by DSP

Assuming negligible nonlinearity, the 4D real electrical waveforms interact with linear channel components represented by their TD 4x4 real transfer matrices consisting of real responses with limited bandwidths (both DSP and devices have limited bandwidth). Following the chronological order of impairments, the 4D received electrical waveforms are $\tilde{r}_t = D_{Rx,t} * R_{4 \times 4}^{OE} * R_{4 \times 4}^{RPN} R_{4 \times 4}^{FO} (h_{4 \times 4}^{CD} * U_{4 \times 4}) * R_{4 \times 4}^{TPN} T_{4 \times 4}^{EO} * D_{Tx,t} * \tilde{t}_t$, where * denotes convolution. For simplicity, first, assume zero electrical crosstalks, $p = \{Tx, Rx\}$, $D_{p,t} = \text{diag}(D_{1,t}^p, D_{2,t}^p, D_{3,t}^p, D_{4,t}^p) \in \mathbb{R}_t^{4 \times 4}$, where the

frequency response of each electrical component, $D_{i,t}^p$, is $D_i^p(\omega) = |D_i^p(\omega)|e^{-j\theta_i^p(\omega)}$. Second, $T_{4 \times 4}^{EO}, R_{4 \times 4}^{OE} \in \mathbb{R}_t^{4 \times 4}$ are the responses of IQ modulators and integrated coherent receiver (ICR), respectively. Third, $R_{4 \times 4}^{pPN}, R_{4 \times 4}^{FO} \in \mathbb{R}_t^{4 \times 4}$ are PN at transmitter (Tx) and receiver (Rx) and FO, respectively, whose entries are real sinusoids in time. Fourth, the bracket indicates that the optical signals experience distributive CD, $h_{4 \times 4}^{CD}$, and polarization effect, $U_{4 \times 4}$, where $U_{4 \times 4}$ is a unitary matrix parameterized by “nearly-static” $a, b, c, d \in \mathbb{R}$ where $a^2 + b^2 + c^2 + d^2 = 1$, i.e., $U_{4 \times 4} * \cong U_{4 \times 4}$.

Rx DSP algorithms are designed to equalize the channel in a “quasi-reverse” order of the impairments: Rx response and quadrature error compensation come first, and optical impairment equalization follows. FO compensation (C) is performed before CDC because $R_{4 \times 4}^{FO}$ and $h_{4 \times 4}^{CD}$ are not commutative (convolution and multiplication do not commute). Signal clocks need to be recovered first via CD compensation before a 2x2 complex MIMO reverses the polarization effect. $h_{4 \times 4}^{CD}$ thus seemingly appears after $U_{4 \times 4}$, but, for small PMD, CD and polarization effects are commutative, i.e., $h_{4 \times 4}^{CD} * U_{4 \times 4} \cong U_{4 \times 4} h_{4 \times 4}^{CD} *$. Carrier phase recovery cannot distinguish Rx PN from Tx PN, resulting in mis-ordered DSP stages and thus equalization enhanced phase noise (EENP)^[4], $R_{4 \times 4}^{EENP}$, and the DSP perceives the channel as if $\tilde{r}_t \cong D_{Rx,t} * R_{4 \times 4}^{OE} * R_{4 \times 4}^{FO} h_{4 \times 4}^{CD} * U_{4 \times 4} R_{4 \times 4}^{EENP} T_{4 \times 4}^{EQ} D_{Tx,t} * \tilde{t}_t$. Finally, $T_{4 \times 4}^{EO} * D_{Tx,t} *$ are compensated by two 2x2 real MIMO equalizers^[2] or 4x4 for XY crosstalks. $T_{4 \times 4}^{EO}, R_{4 \times 4}^{OE}$, are ignored as they can be absorbed into $D_{p,t}$ as crosstalks.

Combine $R_{4 \times 4}^{PN}$ into $R_{4 \times 4}^{FO}$ as they share the same matrix form, the new model becomes $\tilde{r}_t = D_{Rx,t} * R_{4 \times 4}^{FO} (h_{4 \times 4}^{CD} * U_{4 \times 4}) D_{Tx,t} * \tilde{t}_t$ in Fig. 1b or

$$\tilde{r}_t = D_{Rx,t} * R_{4 \times 4}^{FO} (U_{4 \times 4} h_{4 \times 4}^{CD}) * D_{Tx,t} * \tilde{t}_t, \quad (1)$$

With the commutativity between $R_{4 \times 4}^{FO}$ and $U_{4 \times 4}$ (provable by expanding), a back-to-back model becomes, shown in Fig. 1c,

$$\tilde{r}_t = D_{Rx,t} * U_{4 \times 4} R_{4 \times 4}^{FO} D_{Tx,t} * \tilde{t}_t. \quad (2)$$

In this paper, four MIMO equalizer classes will be defined based on their reference locations in Fig. 1d. Their functionalities will be discussed to match some previous DSP designs^{[2],[5-7]} in parameter estimation or calibration.

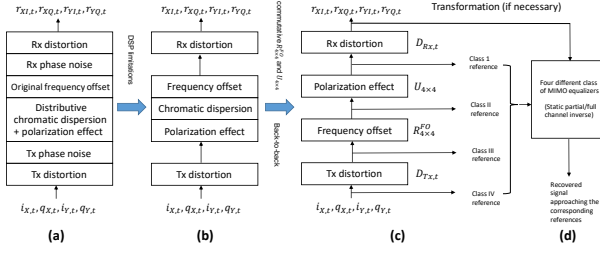


Fig. 1: (a) Channel model (b) Channel model perceived by Rx DSP (c) Simplified model with various reference locations for four equalizer classes (d) Overview of equalization.

Class I: Reference before Rx response

Class I equalizer makes use of the reference signal, $\vec{s}_t = (s_{Xl,t}, s_{XQ,t}, s_{Yl,t}, s_{YQ,t})^T \in \mathbb{R}_t^{4 \times 1}$, taken right after polarization effect shown in Fig.1c, such that $\vec{s}_t = U_{4 \times 4} R_{4 \times 4}^{FO} D_{Tx,t} * \vec{i}_t$, or $\vec{s}_t = D_{Rx,t}^{-1} * \vec{r}'_t$. In experiment, the received signal, $\vec{r}'_t \in \mathbb{R}_t^{4 \times 1}$, where the prime sign represents measurement quantity, convolutes with a 4×4 real MIMO, $\mathbf{h} \in \mathbb{R}_t^{4 \times 4}$. The optimal equalizer can be found using well-known algorithms^[1] to minimize the mean squared error between \vec{s}_t and the equalizer output, i. e., $\mathbf{h}_{opt} := \min_{\mathbf{h}} \| \mathbf{h} * \vec{r}'_t - \vec{s}_t \|^2$. It should approach the inverse of the Rx response, i.e., $\mathbf{h}_{opt} \cong D_{Rx,t}^{-1} \in \mathbb{R}_t^{4 \times 4}$. The reference requires the prior knowledge of Tx impairment and optical channel impairment. Class I equalizer completely characterizes Rx responses. If the Rx impairment is perfectly compensated at the beginning of Rx DSP, a 4×4 real MIMO jointly compensates polarization effect and Tx impairment, which would reduce the overall DSP complexity.

Class II: Reference between $U_{4 \times 4}$ and FO

Class II equalizer takes the reference, \vec{s}_t , between polarization effect and FO such that $\vec{s}_t = R_{4 \times 4}^{FO} D_{Tx,t} * \vec{i}_t \in \mathbb{R}_t^{4 \times 1}$ (in the presence of CD, $\vec{s}_t = R_{4 \times 4}^{FO} h_{4 \times 4}^{CD} * D_{Tx,t} * \vec{i}_t$) or $\vec{s}_t = U_{4 \times 4}^{-1} D_{Rx,t}^{-1} * \vec{r}'_t$. Note that both class I and II employ “FO-rotated references”. In experiment, the received signal, \vec{r}'_t convolutes with a 4×4 real MIMO filter. As an example, if $H_i^p(\omega) = |D_i^p(\omega)|^{-1} e^{j\theta_i^p(\omega)} = e^{-j\omega\tau_i^p}$ is a pure delay filter, the frequency domain (FD) of the optimal 4×4 real equalizer approaches

$$\mathbf{H}_{opt} \cong \begin{bmatrix} ae^{j\omega\tau_1^{Rx}} & -be^{j\omega\tau_2^{Rx}} & ce^{j\omega\tau_3^{Rx}} & -de^{j\omega\tau_4^{Rx}} \\ be^{j\omega\tau_1^{Rx}} & ae^{j\omega\tau_2^{Rx}} & de^{j\omega\tau_3^{Rx}} & ce^{j\omega\tau_4^{Rx}} \\ -ce^{j\omega\tau_1^{Rx}} & -de^{j\omega\tau_2^{Rx}} & ae^{j\omega\tau_3^{Rx}} & be^{j\omega\tau_4^{Rx}} \\ de^{j\omega\tau_1^{Rx}} & -ce^{j\omega\tau_2^{Rx}} & -be^{j\omega\tau_3^{Rx}} & ae^{j\omega\tau_4^{Rx}} \end{bmatrix}. \quad (3)$$

Instead of a 4D real-valued FO-rotated references, equivalently, two complex-valued (X, Y) FO-rotated reference fields, $\vec{s}_{X,t}$, $\vec{s}_{Y,t}$, can also be used:

$$\begin{bmatrix} \vec{s}_{X,t} \\ \vec{s}_{Y,t} \end{bmatrix} = \begin{bmatrix} 1 & j & 0 & 0 \\ 0 & 0 & 1 & j \end{bmatrix} \begin{bmatrix} s_{Xl,t} \\ s_{XQ,t} \\ s_{Yl,t} \\ s_{YQ,t} \end{bmatrix} = \mathbb{G}_{4R \rightarrow 2C} U_{4 \times 4}^{-1} D_{Rx,t}^{-1} * \vec{r}'_t. \quad (4)$$

In experiment, \vec{r}'_t is transformed to, $\vec{r}'_t = (r'_{Xl,t}, j r'_{XQ,t}, r'_{Yl,t}, j r'_{YQ,t})^T$, which is not compulsory

but is recommended to align with^[5] for readers' convenience. \vec{r}'_t convolutes with a 2×4 complex MIMO equalizer (here the MIMO dimension is defined as its matrix dimension). The optimization using the reference fields forces the filter to be complex-valued, approaching the form of, using Eq. (3) and Eq. (4) (let $A = a + jb$, $B = c + jd$):

$$\mathbf{H}_{2 \times 4, opt} \cong \begin{bmatrix} Ae^{j\omega\tau_1^{Rx}} & Ae^{j\omega\tau_2^{Rx}} & Be^{j\omega\tau_3^{Rx}} & Be^{j\omega\tau_4^{Rx}} \\ -B^* e^{j\omega\tau_1^{Rx}} & -B^* e^{j\omega\tau_2^{Rx}} & A^* e^{j\omega\tau_3^{Rx}} & A^* e^{j\omega\tau_4^{Rx}} \end{bmatrix}. \quad (5)$$

Eq. (5) also explains the principle of the well-known 2×4 complex MIMO for joint compensation polarization effect and Rx compensation^[5].

Class III: Reference between FO and Tx

As FO-rotated references are used, the coefficients of class III equalizers are statistic. Starting from class III, let us move the references towards the Tx side by employing “FO-unrotated references”. Thus, the inputs of class III and IV equalizers require FO compensation ahead in order to keep the equalizer coefficients static.

Class III equalizer takes the reference $\vec{s}_{t,o} = D_{Tx,t} * \vec{i}_t = (s_{Xl,o,t}, s_{XQ,o,t}, s_{Yl,o,t}, s_{YQ,o,t})^T \in \mathbb{R}_t^{4 \times 1}$ located after $D_{Tx,t}$ (with Tx impairment only). Recalled that class II reference, \vec{s}_t , is located after $R_{4 \times 4}^{FO}$. Thus, $\vec{s}_{t,o} = (R_{4 \times 4}^{FO})^{-1} \vec{s}_t = (R_{4 \times 4}^{FO})^{-1} U_{4 \times 4}^{-1} D_{Rx,t}^{-1} * \vec{r}'_t$. (With CD, $\vec{s}_{t,o} = (h_{4 \times 4}^{CD})^{-1} * (R_{4 \times 4}^{FO})^{-1} U_{4 \times 4}^{-1} D_{Rx,t}^{-1} * \vec{r}'_t$.) While a static FD channel inverse is desirable for channel estimation or transceiver calibration^[2], $(R_{4 \times 4}^{FO})^{-1} \in \mathbb{R}_t^{4 \times 4}$ that requires multiplication in TD hinders us from moving towards Tx. To avoid using $(R_{4 \times 4}^{FO})^{-1}$, one should perform “field matching”: class II reference fields are FO-compensated to match class III reference fields, i.e., $[\vec{s}_{X,o,t}, \vec{s}_{Y,o,t}]^T = e^{-j\omega\tau_{FO}} [\vec{s}_{X,t}, \vec{s}_{Y,t}]^T$, which is also equivalent to multiplying the FOC phasor elementwise to the 4D class II reference $\vec{s}_t \in \mathbb{R}_t^{4 \times 1}$ as follows,

$$\begin{bmatrix} \vec{s}_{X,o,t} \\ \vec{s}_{Y,o,t} \end{bmatrix} = \mathbb{G}_{4R \rightarrow 2C} \begin{bmatrix} s_{Xl,t} e^{-j\omega\tau_{FO}} \\ s_{XQ,t} e^{-j\omega\tau_{FO}} \\ s_{Yl,t} e^{-j\omega\tau_{FO}} \\ s_{YQ,t} e^{-j\omega\tau_{FO}} \end{bmatrix} = e^{-j\omega\tau_{FO}} \mathbb{G}_{4R \rightarrow 2C} U_{4 \times 4}^{-1} D_{Rx,t}^{-1} * \vec{r}'_t. \quad (6)$$

One may notice that class III channel inverse could look the same as Eq. (4), if the FO can be compensated before Rx response without tremendous loss of optimality, i.e., by assuming

$$\begin{bmatrix} \vec{s}_{X,o,t} \\ \vec{s}_{Y,o,t} \end{bmatrix} \cong \mathbb{G}_{4R \rightarrow 2C} U_{4 \times 4}^{-1} D_{Rx,t}^{-1} * \begin{bmatrix} r'_{Xl} e^{-j\omega\tau_{FO}} \\ r'_{XQ} e^{-j\omega\tau_{FO}} \\ r'_{Yl} e^{-j\omega\tau_{FO}} \\ r'_{YQ} e^{-j\omega\tau_{FO}} \end{bmatrix}. \quad (7)$$

Equivalently, the four received signals are first FO-shifted. In fact, this avoids IQ mixing^[5]. To estimate $U_{4 \times 4}^{-1} D_{Rx,t}^{-1}$, class II equalizer can be re-applied here by using reference fields $\vec{s}_{X,o,t}, \vec{s}_{Y,o,t}$ and with the transformed inputs $\vec{r}'_{t,FOC} = [r'_{Xl,t} e^{-j\omega\tau_{FO}}, j r'_{XQ,t} e^{-j\omega\tau_{FO}}, r'_{Yl,t} e^{-j\omega\tau_{FO}}, j r'_{YQ,t} e^{-j\omega\tau_{FO}}] \in \mathbb{C}_t^{4 \times 1}$, where $\hat{\omega}_{LO}$ is the estimated angular FO. (With CD, the equalizer inputs are $\tilde{h}_{CD}^{-1} \otimes \vec{r}'_{t,FOC} \in \mathbb{C}_t^{4 \times 1}$; \otimes is a

elementwise convolution.) The sub-optimal 2x4 equalizer converges to Eq. (4), when FO is not too large. Compensating FO before the equalizer enables DD-LMS algorithm, which can estimate Rx skew of more than half symbol duration compared to the blind 2x4 CMA equalizer^[5].

Class IV: Tx signal as a reference

Class III does not compensate Tx impairment. Knowing that cascading a 2x2 real MIMO per polarization compensates the Tx impairment^[2], $\tilde{s}_{X,o,t}$ and $\tilde{s}_{Y,o,t}$ should be broken into their real and imaginary parts again. Class III 4D reference, $\tilde{s}_{t,o} \in \mathbb{R}^{4 \times 1}$, can be obtained by

$$\tilde{s}_{t,o} = \underbrace{\begin{bmatrix} S_{XI,o,t} \\ S_{XQ,o,t} \\ S_{YI,o,t} \\ S_{YQ,o,t} \end{bmatrix}}_{\triangleq \mathbb{G}_{4C \rightarrow 4R}} = \frac{1}{2} \begin{bmatrix} 1 & 0 & 1 & 0 \\ -j & 0 & j & 0 \\ 0 & 1 & 0 & 1 \\ 0 & -j & 0 & j \end{bmatrix} \begin{bmatrix} \tilde{s}_{X,o,t} \\ \tilde{s}_{Y,o,t} \\ \tilde{s}_{X,o,t}^* \\ \tilde{s}_{Y,o,t}^* \end{bmatrix}. \quad (8)$$

The reference of class IV can be linked to that of class III by $\tilde{i}_t = D_{Tx,t}^{-1} * \tilde{s}_{t,o}$. By Eq. (7) and Eq. (8),

$$\tilde{i}_t \triangleq D_{Tx,t}^{-1} \mathbb{G}_{4C \rightarrow 4R} \begin{bmatrix} \mathbb{G}_{4R \rightarrow 2C} U_{4 \times 4} D_{Rx,t}^{-1} & \mathbb{O}_{2 \times 4} \\ \mathbb{O}_{2 \times 4} & (\mathbb{G}_{4R \rightarrow 2C} U_{4 \times 4} D_{Rx,t}^{-1})^* \end{bmatrix} * \begin{bmatrix} \tilde{r}_{t,FOC} \\ (\tilde{r}_{t,FOC})^* \end{bmatrix}. \quad (9)$$

This also explains the principle of the 2x8 equalizer^[6], when reference fields, $\mathbb{G}_{4R \rightarrow 2C} \tilde{i}_t$, are used. In experiment, the received signal, \tilde{r}_t' is first transformed to $\tilde{r}_{t,FOC}'$ as if in Class III (without or without CD). Together with its complex-conjugate replicas $(\tilde{r}_{t,FOC}')^* \in \mathbb{C}_t^{4 \times 1}$, the 8 inputs convolute with a 4x8 complex MIMO equalizer, to form the recovered transmitted signal, \tilde{l}_t' . The sub-optimal 4x8 complex MIMO should approach the form of

$$\mathbf{c}_{4 \times 8, opt} \triangleq D_{Tx,t}^{-1} * \mathbb{G}_{4C \rightarrow 4R} \begin{bmatrix} \mathbf{h}_{2 \times 4, opt} & \mathbb{O}_{2 \times 4} \\ \mathbb{O}_{2 \times 4} & \mathbf{h}_{2 \times 4, opt}^* \end{bmatrix}, \quad (10)$$

where $\mathbf{h}_{2 \times 4, opt} \approx \mathbb{G}_{4R \rightarrow 2C} U_{4 \times 4} D_{Rx,t}^{-1}$ is from class II. Eq. (11) is the FD of $\mathbf{c}_{4 \times 8, opt}$, where $\{H_{ij}\}$ are the elements of $\mathbf{H}_{2 \times 4, opt}$ in Eq. (5), $H_{ij}^* \triangleq H_{ij}^*(-f)$, g_i and δ_i are the gain imbalance and phase error factors of four electrical tributaries at Tx. This explains the principle of the joint Tx and Rx IQ FD differential phase extraction^[7]. Classes III and IV are suboptimal due to the assumption Eq. (7).

General Channel Inverse

In the next generation coherent system, more generally, one needs to consider a complex linear system (optical channel) $\mathbb{O}_{2 \times 2} \in \mathbb{C}^{2 \times 2}$ is sandwiched between two real linear systems, $D_{4 \times 4}^{Tx}$, $D_{4 \times 4}^{Rx} \in \mathbb{R}^{4 \times 4}$, in order to optimize each real branch at Tx and at Rx individually. To obtain the overall channel inverse, the immediate complex X, Y fields located between Tx and the optical channel, $\mathbb{O}_{2 \times 2}^{-1} \mathbb{G}_{4R \rightarrow 2C} (D_{4 \times 4}^{Rx})^{-1} * \tilde{r}_t' \in \mathbb{C}_t^{2 \times 1}$, is required to be broken down into their real and imaginary parts (using $\mathbb{G}_{4C \rightarrow 4R}$) in order to connect to the subsequent Tx inverse. Thus, the channel

inverse obtained by an ideal equalizer (if it exists) depends on the complex conjugate replicas of the equalizer inputs:

$$\tilde{l}_t' \triangleq (D_{4 \times 4}^{Tx})^{-1} * \mathbb{G}_{4C \rightarrow 4R} \begin{bmatrix} \mathbb{O}_{2 \times 2}^{-1} \mathbb{G}_{4R \rightarrow 2C} (D_{4 \times 4}^{Rx})^{-1} \tilde{r}_t' & \mathbb{O}_{2 \times 4} \\ \mathbb{O}_{2 \times 4} & (\mathbb{O}_{2 \times 2}^{-1} \mathbb{G}_{4R \rightarrow 2C} (D_{4 \times 4}^{Rx})^{-1} \tilde{r}_t')^* \end{bmatrix} * \begin{bmatrix} \tilde{r}_t' \\ (\tilde{r}_t')^* \end{bmatrix}. \quad (12)$$

Note that the above channel inverse is in its most general form with minimal assumptions (not even EEPN) except nonlinearity. The general channel inverse in Eq. (12) is time-varying due to LO and PN dynamics compared to Class IV's inverse.

Conclusions

Based on a "DSP-perceived" channel model, four classes of MIMO equalizers are presented according to their reference locations. Class I characterizes Rx response. Class II compensates Rx and polarization effects. Class III is class II free of FO dynamics, and it is extended to suboptimal class IV, enabling a complete, static channel inverse from Rx to Tx. Finally, a general channel inverse appears as a time-varying complex-conjugate dependent system which aligns with the widely linear equalization theory.

Acknowledgement

The authors would acknowledge the works of Rios-Müller et al.^[3], and T. Kobayashi et al.^[5] that brought insight to this theoretical work.

References

- [1] S. J. Savory, "Digital filters for coherent optical receivers," Opt. Exp., vol. 16, no. 2, pp. 804–817, 2008.
- [2] C. R. S. Fludger and T. Kupfer, "Transmitter Impairment Mitigation and Monitoring for High Baud-Rate, High Order Modulation Systems," Proc. Eur. Conf. Opt. Commun., 2016, pp. 1-3.
- [3] E. Porto da Silva and D. Zibar, "Widely linear equalization for IQ imbalance and skew compensation in optical coherent receivers," J. Lightw. Technol., vol. 34, no. 15, pp. 3577–3586, 2016.
- [4] W. Shieh and K.-P. Ho, "Equalization-enhanced phase noise for coherent detection systems using electronic digital signal processing," Opt. Exp., vol. 16, no. 20, pp. 15718–15727, 2008.
- [5] R. Rios-Müller et al., "Blind Receiver Skew Compensation and Estimation for Long-Haul Non-Dispersion Managed Systems Using Adaptive Equalizer," J. Lightw. Technol., vol. 33, no.7, pp 1315-1318, 2015.
- [6] T. Kobayashi et al., "35-Tb/s C-band Transmission over 800 km Employing 1-Tb/s PS-64QAM signals enhanced by Complex 8x2 MIMO Equalizer," Opt. Fiber Commun. Conf., 2019, Th4B.
- [7] W. C. Ng, et al., "Joint Transmitter and Receiver IQ Differential Phase Calibration using a single 4x8 MIMO Equalizer", Proc. APC 2021 (SPPCom), SpTh1D.4.

$$\mathbf{c}_{4 \times 8, opt} \triangleq \frac{1}{2} \begin{bmatrix} g_2 e^{-j\delta_2} H_1^x H_{11} & g_2 e^{-j\delta_2} H_1^x H_{12} & g_2 e^{-j\delta_2} H_1^x H_{13} & g_2 e^{-j\delta_2} H_1^x H_{14} & g_2 e^{j\delta_2} H_1^x H_{11} & g_2 e^{j\delta_2} H_1^x H_{12} & g_2 e^{j\delta_2} H_1^x H_{13} & g_2 e^{j\delta_2} H_1^x H_{14} \\ -j g_1 e^{-j\delta_1} H_2^x H_{11} & -j g_1 e^{-j\delta_1} H_2^x H_{12} & -j g_1 e^{-j\delta_1} H_2^x H_{13} & -j g_1 e^{-j\delta_1} H_2^x H_{14} & j g_1 e^{j\delta_1} H_2^x H_{11} & j g_1 e^{j\delta_1} H_2^x H_{12} & j g_1 e^{j\delta_1} H_2^x H_{13} & j g_1 e^{j\delta_1} H_2^x H_{14} \\ g_4 e^{-j\delta_4} H_3^x H_{21} & g_4 e^{-j\delta_4} H_3^x H_{22} & g_4 e^{-j\delta_4} H_3^x H_{23} & g_4 e^{-j\delta_4} H_3^x H_{24} & g_4 e^{j\delta_4} H_3^x H_{21} & g_4 e^{j\delta_4} H_3^x H_{22} & g_4 e^{j\delta_4} H_3^x H_{23} & g_4 e^{j\delta_4} H_3^x H_{24} \\ -j g_3 e^{-j\delta_3} H_4^x H_{21} & -j g_3 e^{-j\delta_3} H_4^x H_{22} & -j g_3 e^{-j\delta_3} H_4^x H_{23} & -j g_3 e^{-j\delta_3} H_4^x H_{24} & j g_3 e^{j\delta_3} H_4^x H_{21} & j g_3 e^{j\delta_3} H_4^x H_{22} & j g_3 e^{j\delta_3} H_4^x H_{23} & j g_3 e^{j\delta_3} H_4^x H_{24} \end{bmatrix}. \quad (11)$$